Kinetic Electron Excitation in Atomic Collision Cascades

S. Meyer,[1] D. Diesing,[2] and A. Wucher[1,*]

[1]*Institute of Experimental Physics, University of Duisburg-Essen, 45117 Essen, Germany*
[2]*Institute of Thin Films and Interfaces (ISG3), Forschungszentrum Jülich, 52425 Jülich, Germany*

(Received 1 March 2004; published 23 September 2004)

The kinetic excitation of electrons upon bombardment of a solid surface with energetic ions is investigated. Using a metal-insulator-metal junction, hot electrons produced by the projectile impact are detected with excitation energies well below the vacuum level. The results provide information that cannot be accessed by electron emission experiments. The observed tunneling current depends on the projectile energy and the bias voltage across the junction, opening the possibility of internal excitation spectroscopy.

DOI: 10.1103/PhysRevLett.93.137601 PACS numbers: 79.20.Rf, 34.50.Dy, 73.40.Rw

If a solid surface is bombarded with energetic particles, the kinetic energy imposed by the projectile is dissipated within the solid by means of elastic collisions (''nuclear stopping'') and electronic excitation processes (''electronic stopping''). For impact energies in the keV range, it is well known that nuclear stopping largely dominates the energy loss experienced by the projectile, thus generating a cascade of atomic subsurface collisions which can ultimately lead to the emission of surface atoms into the gas phase (''sputtering''). Part of the kinetic energy, however, is converted into electronic excitation which manifests, for instance, as the presence of hot electrons in excited states above the Fermi level. If the excitation energy exceeds the work function of the substrate, these electrons can be released into the vacuum, leading to the well-known phenomenon of (kinetic) ion induced electron emission which has been vastly investigated and reviewed several times in the literature [1–4]. In semiconductors and insulators, a similar effect occurs if the excitation energy exceeds the band gap, thus giving rise to conduction band electrons which can then be detected as an internal current.

A major shortcoming of the existing data on ion induced external or internal electron emission is the fact that only those electrons are detected which receive enough energy to overcome a minimum excitation energy of the order of several eV. On the other hand, direct energy transfer by binary projectile-electron collisions, as one of the two prevailing mechanisms of kinetic excitation [4], is expected to produce predominantly low energy excitations. Electron promotion in close collisions between two atoms, as the second possible excitation mechanism [4], may in principle also populate higher lying states, which will, however, quickly relax due to extremely fast electron-electron interaction processes. In a metallic target, both mechanisms will therefore lead to occupation probability distributions peaking at energies close to the Fermi level, a fact which has recently been confirmed by elegant energy loss experiments on fast neutral atoms grazingly scattered from a metal surface [5]. On the basis of presently available experimental data, information on these distributions is restricted to their tails extending above the vacuum level. In order to gain more insight into the excitation and transport mechanisms at lower energies, it is necessary to obtain direct experimental information on hot internal electrons in excited states located between the Fermi and the vacuum levels. To the best of our knowledge, experimental data of that kind are still completely lacking. In the present work, we utilize an internal tunnel junction for the detection of such hot electrons that are produced in the vicinity of an ion bombarded metal surface. More precisely, the target is represented by a thin metallic film which forms one side of a metal-insulator-metal (MIM) system. Excited electrons generated at the surface travel to the metal-oxide interface, tunnel through the thin oxide layer, and are detected as an ion bombardment induced tunneling current in the underlying metal substrate. In order to allow elastic transport between the excitation region and the tunnel junction, the target film thickness must be comparable to the elastic mean free path for electron-electron scattering. On the other hand, the film must be thick enough to prevent significant penetration of projectiles into the underlying oxide layer. A reasonable compromise between these contradicting requirements is found for a film thickness of 20 nm where the penetration probability is calculated [6] to be low (around 10^{-3}) and elastic transport is ensured for excitation energies up to about 1 eV above the Fermi level (see below).

The experiments were carried out in an ultrahigh vacuum system with a base pressure of about 10^{-9} mbar. The primary ions are generated by a commercial rare gas ion source delivering a focused and pulsed ion beam with energies between 5 and 15 keV. The sample is a MIM structure produced by evaporating a thin Al electrode of 20 nm thickness onto an insulating glass substrate. In an electrochemical treatment described in detail elsewhere [7], the Al is locally oxidized to form an Al_2O_3 overlayer of about 2.5 nm thickness. In a third step, a polycrystalline silver layer of 20 nm thickness is vapor

deposited on top of the oxide layer. The two metal electrodes are both 2 mm wide and orientated at 90° with respect to each other (cf. Fig. 1), forming the tunnel junction in the overlap area of 2×2 mm^2. The electrical properties of the junctions produced that way have been carefully characterized previously [7] and were frequently checked during the experiments in order to ensure that, in particular, the oxide layer was not modified due to the ion bombardment.

In a first set of experiments characterizing the electrical response of the system to the ion bombardment, the sample was exposed to a focused and pulsed 10 keV Ar^+ ion beam with a spot size of about 100 μm diameter and a current of 190 nA. The primary ion pulse length was 1–10 ms at a repetition rate of 5 Hz. In order to establish well defined surface conditions, the sample was sputter cleaned using a total ion fluence of about 10^{14} cm^{-2} which ensured that surface adsorbates were removed and no further changes of the measured currents were detected with increasing ion fluence. From the known primary ion current density and background pressure, the remaining surface contamination can be estimated to be in the ppm range. No bias voltage was applied between both electrodes of the MIM system to eliminate any dc current across the junction. The ion beam was aimed at different lateral positions across the layer stack, thus allowing one to bombard the top Ag electrode and the bottom Al electrode separately at positions within and outside the tunneling junction area.

The time dependence of the resulting currents measured on the Al electrode is shown in Fig. 1. First, it is seen that the current transients induced by the projectile ion pulses are clearly discernible. The polarity of the displayed current was chosen such that electrons entering the bottom Al electrode lead to positive values. In Fig. 1(a), the impact point of the beam is located on the Ag electrode at the center of the MIM junction. The positive current pulses observed in this geometry demonstrate that electrons are flowing from the top Ag electrode to the bottom Al electrode, thus indicating a tunneling current of 55 nA across the oxide barrier during the time the ion beam is switched on. When the beam is moved along the Ag electrode to the edge of the MIM junction, the current decreases as displayed in Fig. 1(b), since in this geometry only part of the spot illuminated by the Ar^+ ion beam is located within the junction area. The remaining part of the beam hits the pure Ag film on the glass substrate and therefore does not produce any observable current in the Al electrode. In Fig. 1(c), the spot of the Ar^+ ion beam is still located on the Ag film but completely outside the tunnel junction area, and, hence, no current can be observed. This finding provides clear evidence that the measured signals in Figs. 1(a) and 1(b) are not induced by simple charging effects of the MIM junction capacitance, since such currents would have to appear in the same way for any impact point of the Ar^+ beam on the Ag electrode. In Fig. 1(d) the impact point is located on the Al electrode, far away from the center of the tunnel junction. It is seen that in this case both the sign and the magnitude of the measured current changes as compared to Fig. 1(a). Both findings are expected since now the ion beam hits the bare Al surface and thereby the measured current simply constitutes the beam current.

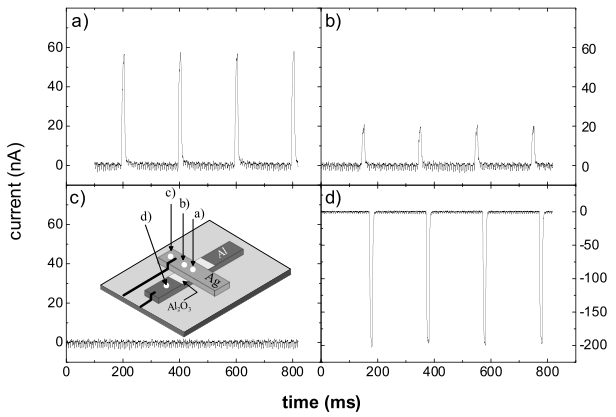

FIG. 1. Current measured through the substrate Al electrode of the MIM junction under ion bombardment. The focused ion beam was aimed at different impact points indicated in the inset.

The tunneling current depicted in Fig. 1(a) is interpreted in terms of projectile ion induced electron excitation at or slightly below the Ag surface. In principle, the source of such excitation can be twofold: First, potential energy carried by the primary ion can be transferred to conduction band electrons, leading to the well-known phenomenon of potential electron emission [8,9]. For the case of singly charged ions, such an excitation process depends only very weakly on the kinetic impact energy of the projectile. Second, kinetic excitation mechanisms as discussed above may lead to direct transfer of kinetic energy to the electronic system. It is clear that these processes must strongly depend on the impact energy of the projectile. In order to differentiate between both excitation mechanisms, Fig. 2 shows the measured tunneling current as a function of the projectile energy. The data have been normalized to the projectile ion current which is given by the measured ion induced total sample current minus the contribution of emitted electrons, the latter being calculated from secondary electron yield values taken from the literature [10]. Again, no bias voltage was applied across the tunnel junction, thus allowing electrons of all excitation states above the Fermi level to contribute to the tunneling current. The results reveal a characteristic which is very similar to that observed in electron emission experiments: At high energies, the signal exhibits a monotonic increase with increasing impact energy, indicating that in this energy range kinetic excitation mechanisms dominate the pro-

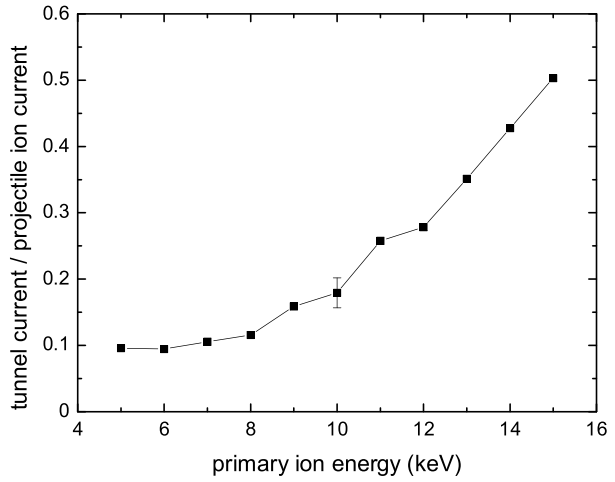

FIG. 2. Tunneling current across the MIM junction as a function of the kinetic energy of the Ar^+ projectile ions impinging onto the Ag surface. The data have been normalized to the projectile ion current and therefore represent the tunneling yield.

duction of hot electrons. At low energies, the signal becomes independent of the impact energy. Note that the kinetic excitation observed in this region may in principle be superimposed by effects induced by the potential (ionization) energy introduced by the impinging projectiles.

A few words are in order discussing the absolute magnitude of the observed tunneling current. From model calculations describing the electronic excitation in collision cascades, we expect a projectile impact to generate a transient excited electron energy distribution with a lifetime of the order of $t_{\mathrm{casc}} \sim 10^{-12}$ s, the properties of which can be coarsely described by an electron temperature of the order of 1500 K [11–13]. The excited electrons are originally produced in a shallow subsurface layer and must travel towards the tunnel junction located at a depth of about 20 nm. The mean free path for electron-electron interaction can be estimated from Fermi liquid theory as [14,15]

$$\lambda_{ee} = \frac{\nu_F}{a(E - E_F)^2 + b(kT_e)^2}, \tag{1}$$

where E is the electron energy and ν_F and E_F denote the Fermi velocity and energy, respectively. For silver, the constants a and b are evaluated as 0.066 $\mathrm{fs}^{-1}\,\mathrm{eV}^{-2}$ [15] and 1.34 $\mathrm{fs}^{-1}\,\mathrm{eV}^{-2}$ [16,17]. At an electron temperature of 1500 K, this allows elastic transport for excitation energies up to approximately 1 eV above the Fermi level. The population of higher states appear depleted at the silver/oxide interface, thus leading to a modified excitation energy distribution characterized by a lower effective electron temperature. Using a mean barrier height E_B, the transmission of the tunnel junction can be estimated as

$$p_t \approx \exp\left(-2\sqrt{\frac{2m_e}{\hbar^2}(E_B - E_\perp)}\, d_{\mathrm{oxide}}\right), \tag{2}$$

where $E_\perp$ denotes the energy associated with the velocity component perpendicular to the tunnel junction. The contribution of excitation states with $E_\perp$ to the measured tunneling current is given by multiplying (2) with the current density across an arbitrary plane in a degenerate electron gas at temperature T_e, which is calculated from the Fermi-Dirac distribution $f(E)$ as [18]

$$j_e(E_\perp) = n_e(E_\perp)\nu_\perp = \frac{n_e}{4\sqrt{E_\perp}} \frac{\int_{E_\perp}^{\infty} f(E)\, dE}{\int_0^\infty \sqrt{E} f(E)\, dE} \sqrt{\frac{2E_\perp}{m_e}}. \tag{3}$$

Here, n_e denotes the overall electron density in the Ag target. For $kT_e \ll E_F$ the normalization integral in the denominator can be approximated as $2/3E_F^{3/2}$. The total tunneling current density is therefore described by

$$j_t = (8m_e)^{-1/2} n_e (\tfrac{2}{3}E_F^{3/2})^{-1} \int_0^\infty \left\{ p_t(E_\perp) \times \int_{E_\perp}^\infty f(E)\, dE \right\} dE_\perp. \tag{4}$$

It is evident that the MIM junction represents an extreme high pass filter which allows only states around or above the barrier top to significantly contribute to the measured signal. The integrand in curly brackets in (4) therefore peaks sharply around the barrier height E_B with a width of approximately $\Delta E \approx 0.2$ eV [19]. In this energy interval, the tunneling probability p_t approaches unity and the double integral in (4) can be roughly approximated by $f(E_B)(kT_e)\Delta E$.

The current density calculated from (4) refers to a steady state situation where the Ag side of the tunnel junction is at T_e and the Al side is at room temperature. In order to calculate the tunneling yield, i.e., the number of detected electrons per projectile impact, we need to acknowledge the limited lifetime and spatial extension of the collision cascade heating the electron gas. The situation described by (4) therefore exists only during the cascade lifetime t_{casc} and within the area A_{casc} after a projectile impact. Hence, the tunneling yield is given by

$$\gamma_t = j_t t_{\mathrm{casc}} A_{\mathrm{casc}} \approx n_e t_{\mathrm{casc}} A_{\mathrm{casc}} (8m_e)^{-1/2} (\tfrac{2}{3}E_F^{3/2})^{-1} f(E_B)(k_B T_e)\Delta E. \tag{5}$$

The magnitude of γ_t can be compared with the measured data of Fig. 2. With $n_e = 5.9 \times 10^{22}$ cm^{-3}, $E_F = 5.5$ eV, $t_{\mathrm{casc}} = 10^{-12}$ s, and $A_{\mathrm{casc}} = (4\ \mathrm{nm})^2$ [20], Eq. (5) yields $\gamma_t \approx 10^3 f(E_B)$, which in connection with $\gamma_t \sim 0.1$ and $T_e \sim 1500$ K results in an effective barrier height of $E_B \sim 1.2$ eV. This value coincides with the barrier heights determined from room temperature ballistic electron

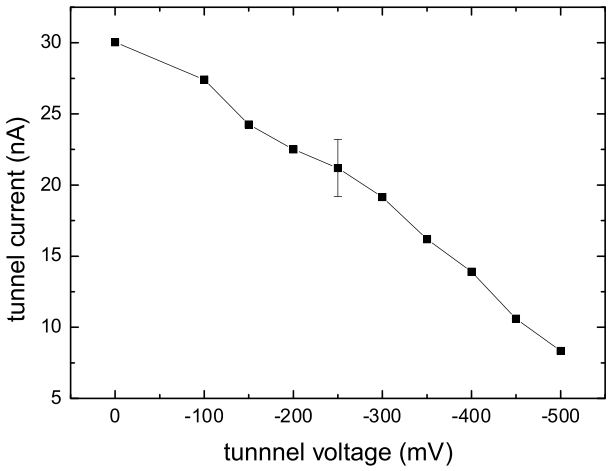

FIG. 3. Projectile induced tunneling current as a function of the bias voltage across the MIM junction. The polarity is selected such as to generate a variable high pass filter which allows only electrons with excitation energies above eV_{bias} to contribute to the measured current.

emission microscopy studies of ultrathin Al oxide tunnel junctions [21,22] and therefore seems reasonable.

So far, all measurements have been performed with zero voltage across the tunnel junction. By applying a negative bias potential to the Al substrate electrode, it is in principle possible to generate an energy dispersive element permitting energy spectroscopy of the excited electrons. As an example, Fig. 3 shows the ion induced part of the measured tunneling current as a function of the bias voltage. The polarity was chosen such as to exclude electrons with excitation energies smaller than eV_{bias} above the Fermi level from contributing to the measured signal. At first sight, the observed signal decrease with increasing V_{bias} appears to be qualitatively expected from the increasing energy discrimination. Because of the high pass filter characteristics of the tunnel junction, however, a quantitative interpretation of the spectrum is highly non trivial. Since the tunneling probability strongly increases with increasing excitation energy, the measured tunneling current is dominated by electrons in states close to the barrier top, and the contribution of those states that are nominally discriminated by V_{bias} is always negligible. As a consequence, the measured bias voltage dependence is essentially determined by subtle changes in the shape of the tunneling barrier. A detailed interpretation of the measured spectrum—involving a fitting procedure of various parameters such as the effective barrier height and asymmetry as well as an effective temperature of the excited electron gas to the bias voltage dependence and absolute magnitude of the measured tunneling current—is outside the scope of this Letter and will be the subject of a forthcoming publication.

In conclusion, we have demonstrated a detection scheme for hot internal electrons excited at a solid surface under bombardment with energetic ions. This is the first experiment exploring the range of low excitation energies which do not lead to electron emission into the vacuum. The results provide new data which complement the large body of experimental data on ion induced electron emission at solid surfaces. Future experiments will include an investigation of the transport by varying the Ag film thickness. Moreover, potential energy effects will be eliminated by neutralizing the primary ion beam.

The authors are greatly indebted to the Deutsche Forschungsgemeinschaft for financial support in the frame of the Sonderforschungsbereich 616 "Energy dissipation at solid surfaces." We also express our gratitude to Jakob Schelten, Angelika Pracht, and Josef Zillekens for assistance during sample preparation.

*Corresponding author.
Email address: wucher@uni-essen.de

[1] D. Hasselkamp *et al.*, *Particle Induced Electron Emission II* (Springer, Berlin, 1992).
[2] W. O. Hofer, Scanning Microsc. **4**, 265 (1990).
[3] B. A. Brusilovsky, Appl. Phys. A **50**, 111 (1990).
[4] R. A. Baragiola, Nucl. Instrum. Methods Phys. Res., Sect. B **78**, 223 (1993).
[5] S. Lederer *et al.*, Phys. Rev. B **67**, 121405 (2003).
[6] The calculation was performed using the SRIM 2003 computer simulation program.
[7] D. Diesing *et al.*, J. Solid State Electrochem. **7**, 389 (2003).
[8] H. D. Hagstrum, in *Chemistry and Physics of Solid Surfaces VII*, edited by R. Vanselow and R. F. Howe (Springer, Berlin, 1988), pp. 341ff.
[9] R. A. Baragiola, in *Low Energy Ion-Surface Interactions*, edited by J.W. Rabalais (Wiley & Sons, Chichester, 1994), pp. 187ff.
[10] R. A. Baragiola *et al.*, Surf. Sci. **90**, 240 (1979).
[11] G. Falcone and Z. Sroubek, Nucl. Instrum. Methods Phys. Res., Sect. B **58**, 313 (1991).
[12] G. Falcone and Z. Sroubek, Phys. Rev. B **38**, 4989 (1988).
[13] A. Duvenbeck *et al.*, Nucl. Instrum. Methods Phys. Res., Sect. B (to be published).
[14] J. J. Quinn, Phys. Rev. **126**, 1453 (1962).
[15] M. Aeschlimann, M. Bauer, and S. Pawlik, Chem. Phys. **205**, 127 (1996).
[16] M. Kaveh and N. Wiser, Adv. Phys. **33**, 257 (1984).
[17] X. Y. Wang *et al.*, Phys. Rev. B **50**, 8016 (1994).
[18] C. B. Duke, *Tunneling in Solids* (Academic Press, London, 1969).
[19] S. Meyer, D. Diesing, and A. Wucher (to be published).
[20] Typical data derived from molecular dynamics computer simulations of the collision cascade.
[21] W. H. Rippard *et al.*, Phys. Rev. Lett. **88**, 046805 (2002).
[22] W. H. Rippard, A. C. Perrella, and R. A. Buhrman, Appl. Phys. Lett. **78**, 1601 (2001).